Canadian Science Publishing
NRC Research Press journals | Publishing Services

Canadian Journal of Chemistry
Revue canadienne de chimie

Analysis of the Interaction between the Cocaine-Binding Aptamer and its Ligands using Fluorescence Spectroscopy

Journal:	*Canadian Journal of Chemistry*
Manuscript ID	cjc-2017-0380.R1
Manuscript Type:	Article
Date Submitted by the Author:	11-Aug-2017
Complete List of Authors:	Shoara, Aron; York University, Chemistry Slavkovic, Sladjana; York University, Chemistry Donaldson, Logan; York University, Biology Johnson, Philip; York University, Chemistry
Is the invited manuscript for consideration in a Special Issue?:	N/A
Keyword:	Fluorescence spectroscopy, fluorescence quenching, aptamers, small molecule-DNA interactions

Analysis of the Interaction between the Cocaine-Binding Aptamer and its Ligands using Fluorescence Spectroscopy

Aron A. Shoara, Sladjana Slavkovic, Logan W. Donaldson & Philip E. Johnson*

Department of Chemistry and Centre for Research on Biomolecular Interactions, York University, Toronto, Ontario, Canada, M3J 1P3.

*To whom correspondence should be addressed. Tel: 1-416-736-2100 x33119; email: pjohnson@yorku.ca

Abstract

We used fluorescence spectroscopy to measure the binding affinity and provide new insights into the binding mechanism of cocaine and quinine with the cocaine-binding DNA aptamer. Using the intrinsic fluorescence of quinine and cocaine, we have observed quenching of ligand fluorescence upon binding of aptamer. Quantification of this quenching provides an easy method to measure the binding constant using small amounts of sample. The observed quenching coupled with a red shift of the Stokes shift in the emission spectrum indicates that quinine and cocaine interact with the aptamer through stacking interactions.

Key words

Fluorescence spectroscopy, fluorescence quenching, aptamers, small molecule-DNA interactions

Introduction

The cocaine-binding aptamer has become a widely employed model system for the development of aptamer-based biosensors. The different sensors, utilizing this aptamer, report ligand binding using a variety of methods including color change, electric and fluorescent outputs amongst numerous other examples.[1-15] The secondary structure of the cocaine-binding aptamer is comprised of a three-way junction with a tandem AG mismatch and a dinucleotide bulge located near the junction (Figure 1).[16] When stem 1 of the aptamer is six base pairs long (MN4, Figure 1) the aptamer is folded both in the free state and the bound state. However, if stem 1 is three base pairs long (MN19, Figure 1) the aptamer is loosely structured in the free state and tightens up or becomes structured upon ligand binding.[16-18] It is this ligand-dependant structural change that is exploited in most of the biosensor applications of this aptamer.

One unusual feature of the cocaine-binding aptamer is that it binds quinine tighter than cocaine, the ligand for which it was originally selected.[19-22] Quinine originated from the bark of the *cinchona* tree and has been widely used for centuries to treat malaria. Quinine was also one of the first fluorophores identified and is a standard for calibrating fluorescence spectrometers.[23] The standard emission spectra of quinine in 1 N H_2SO_4 show that quinine has two excited states at ~250 nm and ~350 nm with one emission state at ~450 nm.[24] The standard fluorescence lifetime (τ) and quantum efficiency (φ) of quinine in 1 N H_2SO_4 are (19.2 ± 0.1) ns and 0.545 ± 0.003, respectively.[25] These standard values can be converted and employed in any experimental condition using a comparative conversion method. [26,27] Cocaine is also fluorescent and absorbs the UV light at 232 nm and 274 nm

while it emits the fluorescent light at 315 nm at room temperature and neutral pH range.[24,28]

In this study, we use the intrinsic fluorescence of both quinine and cocaine to study the binding of quinine and cocaine to two sequence variants of the cocaine-binding aptamer. Fluorescent methods have long been used in aptamer studies but they typically employ a fluorescent tag on the aptamer.[29] To the best of our knowledge this is the first study using the intrinsic fluorescence of a ligand to study aptamer-small molecule interactions. On the basis of our observed fluorescence quenching, as aptamer is added to ligand, the K_d of the aptamer-ligand interaction is measured. From a comparison of the change in fluorescence intensity and Stokes shift observed with ethidium bromide, cocaine and quinine binding we conclude that cocaine and quinine form stacking interactions when binding the aptamer and do not bind via an intercalation mechanism.

Materials and Methods

Sample preparation.

Aptamer samples were obtained from Integrated DNA Technologies (IDT) and had their measured mass confirmed by IDT to be the same as expected using ESI mass spectrometry. The DNA aptamer samples were dissolved in autoclaved distilled deionized H_2O (ddH_2O) and then exchanged three times using a 3-kDa molecular weight cut-off Amicon concentrator with sterilized 2 M NaCl followed by four exchanges into ddH_2O. Quinine hemisulfate monohydrate and cocaine hydrochloride stock powder samples were obtained from Sigma-Aldrich (catalog numbers 145912 and C5776, respectively). Except when it is

specified, all aptamer and ligand samples were dissolved in 20 mM sodium phosphate (pH 7.4), 140 mM NaCl before use. These buffer conditions are similar to what was used in our previous calorimetry-based experiments.[16,20-22] The aptamer and ligand concentrations were determined by a Cary 100 ultraviolet (UV) spectrophotometer using the extinction coefficients supplied by the manufacturers. To avoid the effect of any undesirable quencher species and molecular oxygen all working samples were prepared under sterile conditions, filtered through a 0.2-µm microfilter and degassed with a MicroCal Thermo Vac unit for 5 minutes at 4 °C. To induce the intramolecular folding of MN4, MN19, SS1, MS3 and ATP3 aptamers, DNA samples were incubated at 95 °C for 3 minutes and immediately immersed in ice-water for 5 minutes before they were mixed with the ligand. The sequence of the MS3 aptamer is as published in Neves et al. [30] and the sequence of ATP3 is the same as the 27-mer DNA aptamer published by Lin and Patel.[31]

Fluorescence quenching experiments.

Steady-state fluorescence scans were performed employing a Cary Eclipse spectrofluorometer and 10-mm fused quartz cuvettes. Each experiment was performed at 15 °C and 23 °C. The temperature was maintained constant throughout each experiment using a Cary Peltier controller. Next, the spectrofluorometer was optimized for the limit of detection to maintain constant photomultiplier tube (PMT) voltage, signal-to-noise ratio (SNR) and spectral bandwidth (SBW) parameters. For each ligand-aptamer titration, the total ligand concentration was kept constant and at least half of the expected K_d value. The observed fluorescence intensities from 3-6 replicates were corrected for the inner-filter effect to compensate the loss of the incident intensity by:

$$F = F_{obs} \times 10^{\frac{(A_{ex}+A_{em})\ell}{2}} \quad (1)$$

where F is the corrected fluorescence, F_{obs} is the observed intensity in the absence of the inner-filter effect, A_{ex} and A_{em} are the absorbance values of the aptamer at the excitation and emission wavelengths of the ligand, and (ℓ) is the light path [32,33]. For the simplicity of the parameters referred to in this study, all of the observed fluorescence intensities were corrected and denoted as fluorescence intensity (F). The obtained fluorescence intensities were averaged and normalized as relative fraction units (RFU) of F_0.[34]

For the analysis of 1:1 ligand-aptamer complex, the most valid calculation to quantify the dissociation constant (K_d) is made by a quadratic function:

$$\frac{F_0-F}{F_0-F_b} = \frac{[L]_t+[A]_a+K_d-\sqrt{([L]_t+[A]_a+K_d)^2-4[L]_t[A]_a}}{2[L]_t} \quad (2)$$

where F and F_0 are the fluorescence intensities of the ligand in the presence and absence of the aptamer respectively, F_b is the fluorescence of a fully bound ligand-aptamer, $[L]_t$ is the total concentration of ligand, and $[A]_a$ is the concentration of added aptamer.[33] To quantify the binding affinities, each binding isotherm was plotted as a function of bound to free ligand (F/F_0) versus the total aptamer concentration in the solution. Then, the isotherms were fitted to the non-linear regression function:

$$\frac{F}{F_0} = F_1 + (F_2 - F_1)\frac{K_d^n}{K_d^n+x^n} \quad (3)$$

where n denotes the number of binding sites; F_2 and F_1 are the vertical and horizontal asymptotes respectively. The K_d in Eq. 3 is derived from the quadratic binding function (Eq.

2).[33] The fitting model (Eq. 3) was defined and developed applying OriginPro 2016 C scripts.

In the quinine-aptamer binding assays, quinine was excited at 234 nm. Then, emission scans were performed from 270 nm to 450 nm to exclude the interference of Raman and Rayleigh scattering peaks, and to detect the maximum fluorescence intensity of quinine at ~383 nm. For the cocaine-aptamer binding assays, cocaine was excited at 232 nm. The emission scans were carried out from 270 nm to 450 nm, and the maximum fluorescence intensity of cocaine was detected at ~315 nm. To confirm the quenching results were specific for a functional cocaine-binding aptamer, both ligands were titrated against the non-binding SS1 aptamer at 15 °C and under the same conditions performed for MN4 and MN19.

In the dynamic quenching analyses, the Stern-Volmer isotherms of the acquired maximum fluorescence intensities were plotted as a function of free to bound ligand (F_0/F) versus the total aptamer concentration. The Stern-Volmer plots were fitted to the mixed static-dynamic quenching models:

$$\frac{\mathrm{F_0}}{\mathrm{F}} = (1 + K_{\mathrm{SV}}[\mathrm{Q}])(1 + K_{\mathrm{a}}[\mathrm{Q}]) \quad (4)$$

$$\frac{\mathrm{F_0}}{\mathrm{F}} = (1 + K_{\mathrm{SV}}[Q])e^{V[Q]} \quad (5)$$

where the association constant (K_{a}) and the Stern-Volmer constant (K_{SV}) become mutually dependent constants, and (V) stands for the volume per mole of the ligand-aptamer complex within the static interaction proximity.[35-37]

To compare the effect of intercalation versus base-stacking interactions, the MN4 and MN19 aptamers were titrated into 1 μM ethidium bromide and excited at 230 nm, 286 nm and 486 nm separately. Each emission scan was acquired from 550 to 700 nm to detect the fluorescence of ethidium bromide at ~613 nm at 23 °C. Similar to binding affinity analyses of quinine and cocaine, the maximum emitted intensities of ethidium bromide were averaged, corrected and analyzed as ratios to F_0. Furthermore, wavelengths of the emission maxima were recorded to determine the Stokes shift of each fluorescence scan. The difference in Stokes shifts between free and bound states ($\Delta\lambda_b^f$) of the ligands (ethidium bromide, quinine and cocaine) with the MN4 and MN19 aptamers were noted for comparison analyses.

To quantify the bimolecular quenching rate constant (k_q) of cocaine, the fluorescence lifetime (τ) of cocaine in the absence of aptamers were measured using the time-resolved mode of the Cary Eclipse spectrofluorometer at 15 °C and 23 °C. The rate of the fluorescence intensity as a function of time (t) was fitted to

$$F(t) = I_0 e^{-t/\tau} \quad (6)$$

where I_0 denotes the incident light intensity[23]. For the calculation of k_q in quinine-aptamer binding experiments, we used the standard τ_0 values available in the literature (18.5 ns and 17.5 ns) at 15 °C and 23 °C respectively.[25] The k_q was computed using:

$$\frac{F_0}{F} = 1 + K_{SV}[Q] = 1 + K_a[Q] = 1 + k_q\tau_0[Q] \quad (7)$$

where the Stern-Volmer constant (K_{SV}) represents a dynamic binding constant in a collisional interaction. In an exclusively static quenching, the K_{SV} is replaced with the K_a.[38,39]

Results

Effect of aptamer binding on ligand fluorescence.

Upon addition of aptamer to quinine or cocaine, the fluorescence of the ligand was quenched (Figure 2). We utilized this quenching to quantify the binding affinity and dynamics of MN4 and MN19 to both quinine and cocaine. The observed fluorescence emission maxima were corrected for the inner-filter effect using Eq. 1 for each aptamer-ligand pair accounting for the absorbance of DNA at the excitation wavelength used for the ligand (Supporting Figure 1). We found that the titrations of MN4 and MN19 into a constant concentration of quinine, while irradiated at 234 nm, quenched the maximum fluorescence emission at ~383 nm (Figure 2a). Similarly, the titrations of MN4 and MN19 aptamers in cocaine, while excited at 232 nm, quenched the maximum fluorescence emission at ~315 nm (Figure 2b). The nonlinear fitting analyses of the acquired binding isotherms using Eq. 3 (Figure 3) yielded the K_d values reported in Table 1. The K_d values of all four aptamer-ligand combinations decreased as the temperature was raised from 15 °C to 23 °C (Table 1).

In order to confirm that the fluorescence quenching we observe is a result from specific binding, we analysed the change in fluorescence of quinine and cocaine upon addition of the SS1 cocaine-binding aptamer. This aptamer has the same sequence as MN4 except that both AG bases (A21/G29, A7/G30) are switched to be GA base pairs (G21/A29, G7/A30)

(Figure 4a). These two changes result in an aptamer that does not bind to quinine as assessed by ITC methods (Figure 4b). When SS1 was titrated into cocaine or quinine, the observed fluorescence reduced in intensity; however, when corrected for the inner filter effect no reduction in binding was observed (Figure 4c, d). As a comparison, the observed and corrected data for MN4-quinine is also shown in Figure 4e. As a further control we tested the MS3 and ATP3 DNA sequences as additional negative controls for binding and also observed no change in the observed fluorescence upon addition of MN4 (Supporting Figure 2).

The shift of the emission maximum of quinine was measured in the free and ligand-bound states for both MN19 and MN4 aptamers. When quinine was bound by MN4, the emission maxima of quinine shifted (3.05 ± 0.02) nm toward the infrared region (Figure 5). A slightly shorter red shift of (2.49 ± 0.01) nm occurred when quinine was bound by MN19. With cocaine binding, the emission maximum of MN4•cocaine shifted (1.07 ± 0.03) nm toward the infrared region, and with MN19 red-shifted by (0.46 ± 0.01) nm (Figure 5). These differences in Stokes shift are statistically different as confirmed by a t-test with a p-value less than 0.0001.

To provide a comparison for quinine and cocaine binding, we titrated MN4 and MN19 into ethidium bromide (EtBr) and monitored the change in fluorescence of EtBr. When bound by both MN4 and MN19, the fluorescence intensity of EtBr increased (Figure 5b). Additionally, the MN4•EtBr and MN19•EtBr complexes resulted a blue shift in the EtBr emission spectrum of (10.9 ± 0.02) nm and (11.5 ± 0.1) nm, respectively (Figure 5).

As a control ligand binding we also analysed the interaction of benzoylecgonine with MN4. Benzoylecgonine is a metabolite of cocaine and the cocaine-binding aptamer is typically described as only weakly binding or not interacting with this molecule.[1,21,40,41] Using differential scanning calorimetry (DSC) methods Harkness and coworkers have determined an affinity of MN4 for benzoylecgonine of 604 μM at 30 °C.[22] Benzoylecgonine has the same fluorescent properties as cocaine and as shown in Supporting Figure 3 its fluorescence is quenched upon addition of MN4 with a resulting K_d value of (91 ± 52) μM at 15 °C. This binding affinity agrees reasonably well with the expected affinity of 220 μM that is calculated using the thermodynamic parameters previously reported.[22] We will also note that the lower K_d value measured here at a lower temperature is consistent with our binding measurements that show that the affinity of the cocaine-binding aptamer increases as the temperature is decreased (Table 1).

Analysis of fluorescence quenching mechanisms.

We analyzed the mechanism of the fluorescence quenching of quinine and cocaine with MN4 and MN19 binding by Stern-Volmer analysis. The Stern-Volmer isotherm of MN4-quinine at 15 °C produced a non-linear plot with K_{sv} constant of (7.2 ± 0.3) μM^{-1}, using the linear portion of the binding curve. The isotherm saturated with excess MN4 indicating that the ligand is fully bound (Figure 6a). In contrast, at 23 °C the MN4-quinine titration resulted in a linear Stern-Volmer plot with K_{sv} constant of (1.31± 0.03) μM^{-1} (Figure 6a). As both of these plots have a linear region, when the temperature is increased, the K_{sv} value decreases. Therefore, we conclude that the MN4-quinine quenching follows a static

mechanism.[35,38,39,42]

The titrations of MN4-cocaine at 15 °C and 23 °C showed non-linear Stern-Volmer plots with K_{SV} constants of (0.24 ± 0.02) μM^{-1} and (0.11 ± 0.00) μM^{-1}, respectively (Figure 6b). The titrations of MN19-quinine at 15 °C and 23 °C also showed non-linear Stern-Volmer plots with K_{SV} constants of (2.71 ± 0.06) μM^{-1} and (0.81 ± 0.01) μM^{-1}, respectively (Figure 6c). For both of these aptamer-ligand pairs, the curve shows that quenching occurs through a mixed static-dynamic process.[35,38,39,42]

For the titration of MN19 with cocaine at 15 °C, we observe a linear Stern-Volmer plot with a K_{SV} constant of $(3.4 \pm 0.06) \times 10^{-3}$ μM^{-1}. We obtain non-linear plot with K_{SV} constant of $(4.75 \pm 0.06) \times 10^{-3}$ μM^{-1} at 23 °C (Figure 6d). This switch from a linear to a quadratic plot and an increase in K_{sv} value with temperature indicates that the quenching mechanism changes from a mostly static to a mostly dynamic mechanism.

The fluorescence lifetime (τ) of free cocaine was measured using time-resolved fluorescence spectroscopy. For free cocaine, τ was measured to be (2.56 ± 0.73) μs and (2.23 ± 0.83) μs at 15 °C and 23 °C, respectively (Supporting Figure 4). Using the τ value the bimolecular quenching rate constants (k_q) for cocaine was determined using eq. 7 and reported in Table 1. For quinine, the τ value is too short to measure using our instrumentation. Instead, we used the τ values of quinine available in the literature[25] to quantify the k_q values of quinine interacting with MN19 and MN4 (Table 1).

Discussion

We have used the observed fluorescence quenching of quinine and cocaine with aptamer binding to measure the affinity of these ligands to both the MN4 and MN19 cocaine-binding aptamer constructs (Table 1). The values measured here agree within experimental error with our previously reported values using ITC values.[16,21,30] The benefits of using this fluorescence technique to measure binding affinity are the significantly (over 40 fold) lower amounts of material needed for fluorescence methods compared to ITC methods, and the faster time it takes perform the titration in the fluorescence experiment than in the ITC run (though the ITC experiment is automated). The experiment performed in this study, where the intrinsic change in fluorescence intensity upon binding is used to measure affinity, is not new but has rarely been used to study aptamer-ligand interactions. This method should be easily implemented to other aptamer-ligand pairs as long as the ligand for the aptamer has fluorescence properties.

The fluorescence studies performed here also provide new insights into the binding interaction of cocaine and quinine with the cocaine-binding aptamer. As we previously noted,[20] the values of the thermodynamic binding parameters (ΔH and $T\Delta S$) place cocaine and quinine into the intercalating-type of DNA ligands as classified by Chaires [43]. However, quinine and cocaine are not known to be intercalating molecules, nor do they seem likely to be intercalators as their structures possess only one or two fused aromatic rings. Instead, we have thought that these two ligands interact with the cocaine-binding aptamer in a stacking manner where one face of the aromatic ring of the ligand interacts in a π–π

stacking manner with a base or multiple bases in the aptamer. It is likely that stacking interaction contribute significantly to binding as 6-methoxyquinoline, the aromatic portion of quinine, is bound by the cocaine-binding aptamer ten-fold tighter than cocaine.[21]

In support of this stacking mechanism, we measured the fluorescence binding properties of a known intercalator, ethidium bromide, and compared them with those of cocaine and quinine. The fluorescence intensity of ethidium bromide increases when bound by the aptamer and we observe a blue shift of 11-12 nm with MN4 and MN19 binding (Figure 5). These values are consistent with previously reported changes in fluorescence for ethidium brominde intercalating into DNA.[44,45] In contrast, cocaine and quinine exhibit fluorescence quenching and a red shift when binding MN19 or MN4 (Figure 5). These differences indicate that in the bound state, quinine and cocaine are still at least partially solvent accessible as would be expected in a stacking arrangement. Jagtep *et al*. demonstrated that overlap of conjugated π-systems in stacking interactions results in a distinctive emission transition to the low-energy range, and this red shift increases with greater π-system overlap.[46] Our results show that quinine binding by MN19 and MN4 yields a greater red shift than when the same aptamers bind cocaine. Detecting a smaller red shift in cocaine-aptamer emission spectra corresponds to cocaine having one aromatic ring as opposed to two fused aromatic rings in quinine. This is consistent with stacking interactions.

To conclude, the change in the fluorescence spectrum of quinine and cocaine ligands as a function of cocaine-binding aptamer concentration is a powerful and sensitive tool to

295 quantify the binding affinities of cocaine-binding aptamers as well as providing insights
296 into their binding mechanisms.

297

298

Acknowledgment

We thank Ekaterina Smirnova (York University) for help with the use of the spectrofluorometer as well as past and present members of the Johnson laboratory for useful discussions.

References

(1) Stojanovic, M. N.; de Prada, P.; Landry, D. W. *J. Am. Chem. Soc.* **2000**, *122*, 11547.

(2) Stojanovic, M. N.; Landry, D. W. *J. Am. Chem. Soc.* **2002**, *124*, 9678.

(3) Baker, B. R.; Lai, R. Y.; Wood, M. S.; Doctor, E. H.; Heeger, A. J.; Plaxco, K. W. *J. Am. Chem. Soc.* **2006**, *128*, 3138.

(4) Liu, J.; Lu, Y. *Angew. Chem., Int. Ed.* **2006**, *45*, 90.

(5) Shlyahovsky, B.; Li, D.; Weizmann, Y.; Nowarski, R.; Kotler, M.; Willner, I. *J. Am. Chem. Soc.* **2007**, *129*, 3814.

(6) Chen, J.; Jiang, J.; Gao, X.; Liu, G.; Shen, G.; Yu, G. *Chem. - Eur. J.* **2008**, *14*, 8374.

(7) Freeman, R.; Sharon, E.; Tel-Vered, R.; Willner, I. *J. Am. Chem. Soc.* **2009**, *131*, 5028.

(8) Xiang, Y.; Lu, Y. *Nature Chem.* **2011**, *3*, 697.

(9) Kawano, R.; Osaki, T.; Sasaki, H.; Takinoue, M.; Yoshizawa, S.; Takeuchi, S. *J. Am. Chem. Soc.* **2011**, *133*, 8474.

(10) Kang, K.; Sachan, A.; Nilsen-Hamilton, M.; Shrotriya, P. *Langmuir* **2011**, *27*, 14696.

(11) Sharma, A. K.; Heemstra, J. M. *J. Am. Chem. Soc.* **2011**, *133*, 12426.

(12) Das, J.; Cederquist, K. B.; Zaragoza, A. A.; Lee, P. E.; Sargent, E. H.; Kelley, S. O. *Nature Chem.* **2012**, *4*, 642.

(13) Malile, B.; Chen, J. I. *J. Am. Chem. Soc.* **2013**, *135*, 16042.

(14) Roncancio, D.; Yu, H.; Xu, X.; Wu, S.; Liu, R.; Debord, J.; Lou, X.; Xiao, Y. *Anal. Chem.* **2014**, *86*, 11100.

(15) Neves, M. A. D.; Blaszykowski, C.; Bokhari, S.; Thompson, M. *Biosens. Bioelectron.* **2015**, *72*, 383.

(16) Neves, M. A. D.; Reinstein, O.; Johnson, P. E. *Biochemistry* **2010**, *49*, 8478.

(17) Neves, M. A. D.; Slavkovic, S.; Churcher, Z. R.; Johnson, P. E. *Nucleic Acids Res.* **2017**, *45*, 1041.

(18) Churcher, Z. R.; Neves, M. A. D.; Hunter, H. N.; Johnson, P. E. *J. Biomol. NMR* **2017**, *68*, 33.

(19) Pei, R.; Shen, A.; Olah, M. J.; Stefanovic, D.; Worgall, T.; Stojanovic, M. N. *Chem. Commun.* **2009**, 3193.

(20) Reinstein, O.; Yoo, M.; Han, C.; Palmo, T.; Beckham, S. A.; Wilce, M. C. J.; Johnson, P. E. *Biochemistry* **2013**, *52*, 8652.

(21) Slavkovic, S.; Altunisik, M.; Reinstein, O.; Johnson, P. E. *Bioorg. Med. Chem.* **2015**, *23*, 2593.

(22) Harkness V, R. W.; Slavkovic, S.; Johnson, P. E.; Mittermaier, A. K. *Chem. Commun.* **2016**, *52*, 13471.

(23) Lakowicz, J. R. *Principles of Fluorescence Spectroscopy*; 3 ed.; Springer, 2006.

(24) Sangster, A. W.; Stuart, K. L. *Chem. Rev.* **1965**, *65*, 69.

(25) Velapeidi, R. A.; Mieinz, K. D. *A fluorescence standard reference material: Quinine sulfate dihydrate* Washington DC, 1980.

(26) Drushel, H. V.; Sommers, A. L.; Cox, R. C. *Anal. Chem.* **1963**, *35*, 2166.

(27) Birks, J. B. *J. Res. NBS A Phys. Ch.* **1976**, *80A*, 389.

(28) Mercolini, L.; Mandrioli, R.; Saladini, B.; Conti, M.; Baccini, C.; Raggi, M. A. *J. Pharm. Biomed. Anal.* **2008**, *48*, 456.

(29) Du, Y.; Dong, S. *Analytical chemistry* **2017**, *89*, 189.

(30) Neves, M. A. D.; Reinstein, O.; Saad, M.; Johnson, P. E. *Biophys. Chem.* **2010**, *153*, 9.

(31) Lin, C. H.; Patel, D. J. *Chem. Biol.* **1997**, *4*, 817.

(32) Van De Weert, M. *J. Fluoresc.* **2010**, *20*, 625.

(33) Van De Weert, M.; Stella, L. *J. Mol. Struct.* **2011**, *998*, 145.

(34) Gutow, J. H. *J. Chem. Educ.* **2005**, *82*, 302.

(35) Eftink, M. R.; Ghiron, C. A. *Anal. Biochem.* **1981**, *114*, 199.

(36) Laws, W. R.; Contino, P. B. *Methods Enzymol.* **1992**, *210*, 448.

(37) Mocz, G.; Ross, J. A. *Methods in Molecular Biology: Protein-Ligand Interactions*; 2 ed.; Springer-Humana: Hatfield, UK, 2013; Vol. 1008.

(38) Eftink, M. R.; Ghiron, C. A. *Proc. Natl. Acad. Sci. USA* **1975**, *72*, 3290.

(39) Stern, O.; Volmer, M. *Phys. Z* **1919**, *20*, 183.

(40) Stojanovic, M. N.; de Prada, P.; Landry, D. W. *J. Am. Chem. Soc.* **2001**, *123*, 4928.

(41) Bozokalfa, G.; Akbulut, H.; Demir, B.; Guler, E.; Gumus, Z. P.; Odaci Demirkol, D.; Aldemir, E.; Yamada, S.; Endo, T.; Coskunol, H.; Timur, S.; Yagci, Y. *Anal. Chem.* **2016**, *88*, 4161.

(42) Blatt, E.; Chatelier, R. C.; Sawyer, W. H. *Biophysical journal* **1986**, *50*, 349.

(43) Chaires, J. B. *Annu. Rev. Biophys.* **2008**, *37*, 135.

(44) Jenkins, T. C.; 1 ed.; Fox, K. R., Ed.; Springer-Humana: Totowa, NJ, 1998; Vol. 90, p 195.

(45) Garbett, N. C.; Hammond, N. B.; Graves, D. E. *Biophys. J.* **2004**, *87*, 3974.

(46) Jagtap, S. P.; Mukhopadhyay, S.; Coropceanu, V.; Brizius, G. L.; Brédas, J. L.; Collard, D. M. *J. Am. Chem. Soc.* **2012**, *134*, 7176.

371 **Tables**
372

Table 1. Dissociation constants and binding parameters of quinine and cocaine with the MN4 and MN19 aptamers constructs.[1]

Ligand	Aptamer	T (°C)	K_d (μM)	K_{SV} (μM^{-1})	k_q (μM^{-1}s^{-1})
Quinine	MN4	15.0	0.094 ± 0.003	7.2 ± 0.3	3.91×10^{8}
		23.0	0.745 ± 0.004	1.31 ± 0.03	7.08×10^{7}
	MN19	15.0	0.47 ± 0.01	2.71 ± 0.06	1.46×10^{8}
		23.0	1.09 ± 0.02	0.81 ± 0.01	4.39×10^{7}
Cocaine	MN4	15.0	3.92 ± 0.07	0.24 ± 0.02	1.55×10^{1}
		23.0	7.7 ± 0.1	0.11 ± 0.00	7.10×10^{0}
	MN19	15.0	21.1 ± 0.6	$(3.4 \pm 0.9) \times 10^{-3}$	2.19×10^{-1}
		23.0	28.8 ± 0.3	$(4.75 \pm 0.06) \times 10^{-3}$	3.10×10^{-1}

[1] Assays carried out in 20 mM sodium phosphate buffer (pH 7.4), and 140 mM NaCl. The error range stated here is the standard deviation after fitting to a mean of three to six replicates.

373
374

Figure Captions

Figure 1. Structures of the ligands and the DNA aptamers used in this study. Dashed lines between nucleotides indicate Watson-Crick base-pairing in the secondary structure whereas diamonds show the AG base pairs. Solid lines display the phosphodiester bonds in the backbone of the aptamers.

Figure 2. The raw fluorescence emission spectra of (a) quinine and (b) cocaine titrated with the MN4 aptamer. Fluorescence scans were carried out in 20 mM sodium phosphate buffer (pH 7.4), and 140 mM NaCl at 23 °C. Aptamer aliquots quenched fluorescence, and aptamer was added until the fluorescence of the ligand remained unchanged between additions. (**a**) Fluorescence emission spectra of 0.06 μM quinine hemisulfate excited at 234 nm. (**b**) Fluorescence emission spectra of 4.8 μM cocaine hydrochloride excited at 232 nm.

Figure 3. Steady-State fluorescence quenching analysis of quinine and cocaine ligands binding MN4 and MN19 aptamers in 20 mM sodium phosphate, (pH 7.4) 140 mM NaCl at 15 °C (blue triangle) and 23 °C (red square). Displayed here are the titrations of (**a**) MN4-quinine; (**b**) MN4-cocaine; (**c**) MN19-quinine and (**d**) MN19-cocaine. The corrected and normalized relative fraction fluorescence (RFU) for each ligand is expressed on the y-axis, where F_0 and F are inner-filter corrected emission maxima in the absence and presence of the corresponding aptamer. Each data point represents an average of 3-6 experiments with the error bar representing one standard deviation.

Figure 4. Putative secondary structure of the SS1 aptamer construct (**a**). This aptamer has the tandem AG base pairs as typically seen in the functional cocaine-binding aptamer changed to be GA base pairs. Isothermal titration calorimetry (ITC) experiment (**b**) where the SS1 aptamer is titrated with quinine shows no ligand binding occurs with this aptamer. ITC data was acquired in 20 mM sodium phosphate (pH 7.4) 140 mM NaCl at 20 °C. Negative control titration of the non-binding aptamer SS1 with quinine and cocaine at 15 ˚C. Shown is the emission of cocaine (**c**) and quinine (**d**) ligands versus SS1 aptamer concentration in 20 mM sodium phosphate (pH 7.4) and 140 mM NaCl. The blue diamonds show the observed non-specific quenching of fluorescence due to the inner-filter effect of the aptamer. The red circles are the corrected fluorescence using Eq. 3. Isotherms in (**e**) display a comparison between the observed and corrected fluorescence quenching in MN4-quinine.

Figure 5. The fluorescence emission spectra of quinine and ethidium bromide titrated with MN4. Fluorescence scans were carried out in 20 mM sodium phosphate buffer (pH 7.4), and 140 mM NaCl at 23 °C. Aptamer aliquots were added until the fluorescence of the ligand remained unchanged. (**a**) Fluorescence emission spectra of 0.06 μM quinine hemisulfate excited at 234 nm. (**b**) Fluorescence emission spectra of 1 μM ethidium bromide excited at 230 nm. (**c**) Bar graph of the change in Stokes shift for the indicated combinations of ligand and aptamer.

Figure 6. Dynamic and static fluorescence quenching analysis of quinine and cocaine ligands binding MN4 and MN19 aptamers at 15 °C (blue triangles) and 23 °C (red squares).

421 Shown here are the Stern-Volmer plots of (**a**) MN4-quinine; (**b**) MN4-cocaine; (**c**) MN19-
422 quinine and (**d**) MN19-cocaine. The corrected and normalized relative fraction
423 fluorescence (RFU) for each ligand is expressed on the y-axis, where F_0 and F are inner-
424 filter corrected emission maxima in the absence and presence of the corresponding
425 aptamer. Each data point represents an average of 3-6 experiments with the error bar
426 representing one standard deviation.
427

428 **Graphical Abstract**

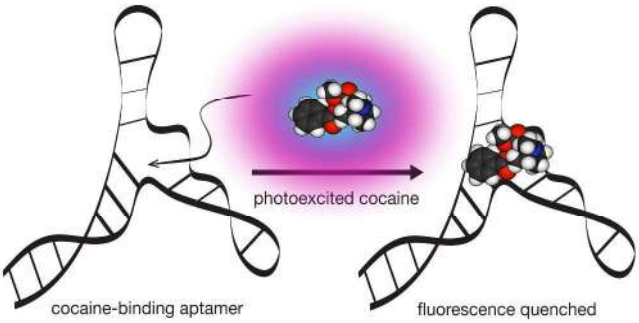

429

Supporting Information

Figure S1. The spectral overlap of unbound ligands and aptamers examined in this study. Spectra on left are the normalized UV absorbance of (**a**) MN19, and (**c**) MN4 aptamers in arbitrary units (a.u.). Spectra on right are the normalized emission fluorescence of (**b**) free cocaine, and (**d**) free quinine. All data acquired in 20 mM sodium phosphate (pH 7.4) 140 mM NaCl at 23 °C. Quinine emission spectrum does not overlap with the absorbance spectra of aptamers whereas cocaine emission spectrum overlaps with the absorbance spectra of aptamers.

Figure S2. Negative control titrations of the non-binding MS3 (black squares) and ATP3 (red circles) aptamers with quinine at 15 °C. Shown is the emission of quinine versus aptamer concentration in 20 mM sodium phosphate (pH 7.4) and 140 mM NaCl. The data shown is the corrected fluorescence using Eq. 3.

Figure S3. Steady-State fluorescence quenching analysis of benzoylecgonine binding MN4 in 20 mM sodium phosphate, (pH 7.4) 140 mM NaCl at 15 °C. The corrected and normalized relative fraction fluorescence (RFU) for the ligand is shown on the y-axis, where F_0 and F are inner-filter corrected emission maxima in the absence and presence of the corresponding aptamer. Each data point represents an average of 3 experiments with the error bar representing one standard deviation.

Figure S4. Fluorescence time-resolved analysis of unbound cocaine. Shown are the fluorescence lifetime decay of cocaine in 20 mM sodium phosphate (pH 7.4) 140 mM NaCl

453 at 15 °C (blue) and 23 °C (red). The lifetime measured (2.56 ± 0.73) μs and (2.23 ± 0.83) μs
454 at 15 °C and 23 °C respectively.
455
456

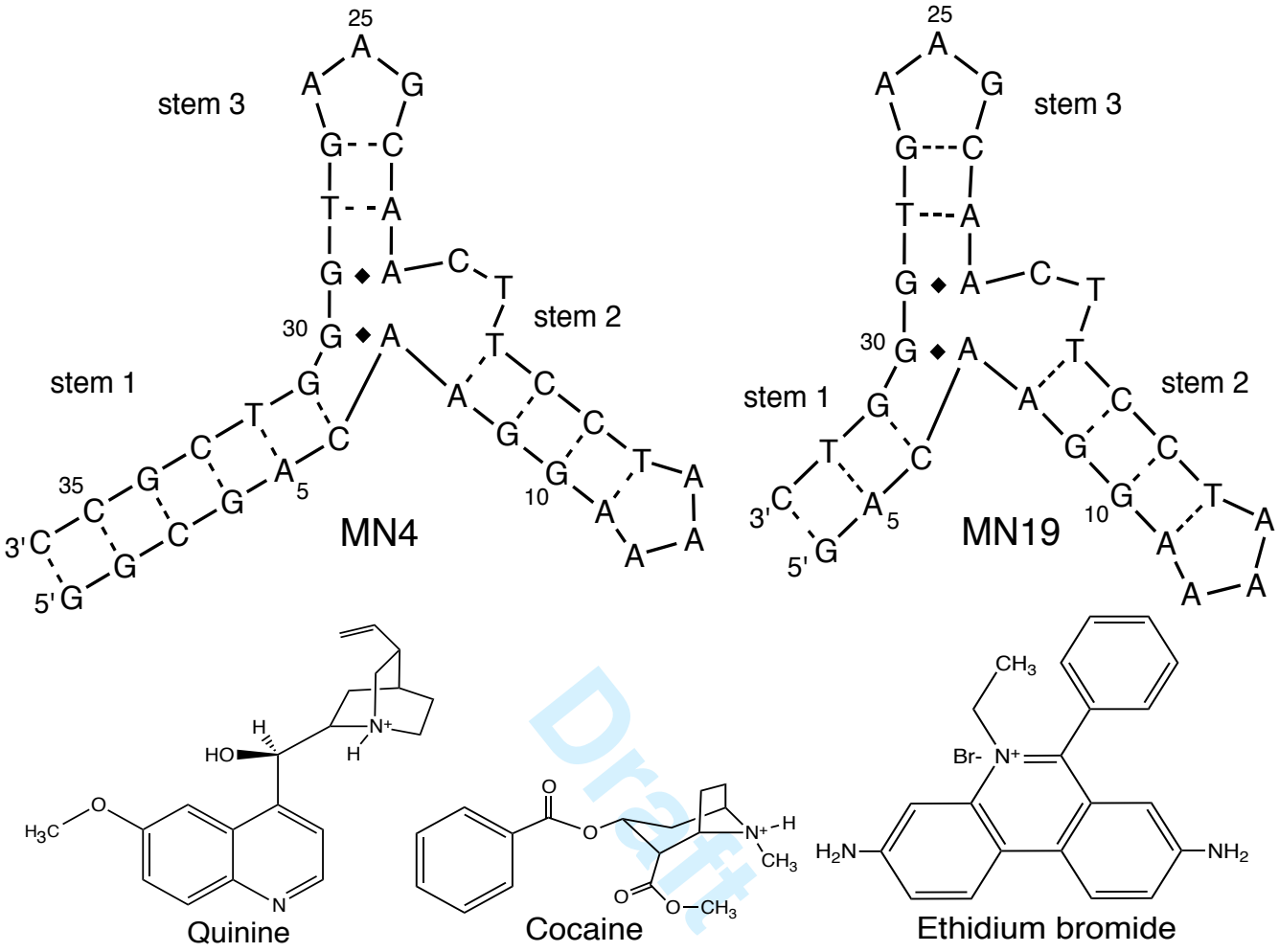

Figure 1

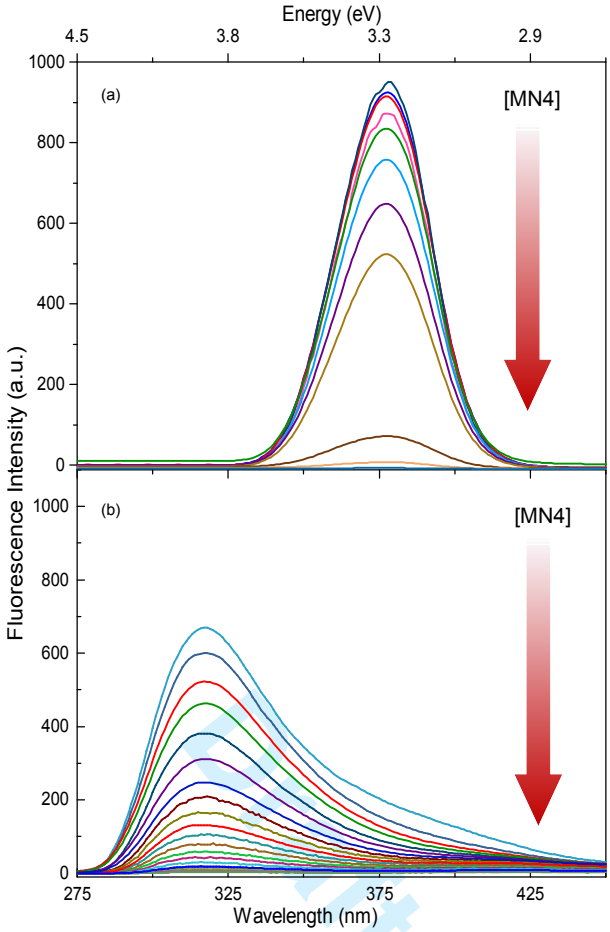
Energy (eV)
4.5
3.8
3.3
2.9
(a)
[MN4]
(b)
[MN4]
Fluorescence Intensity (a.u.)
0
200
400
600
800
1000
275
325
375
425
Wavelength (nm)

Figure 2

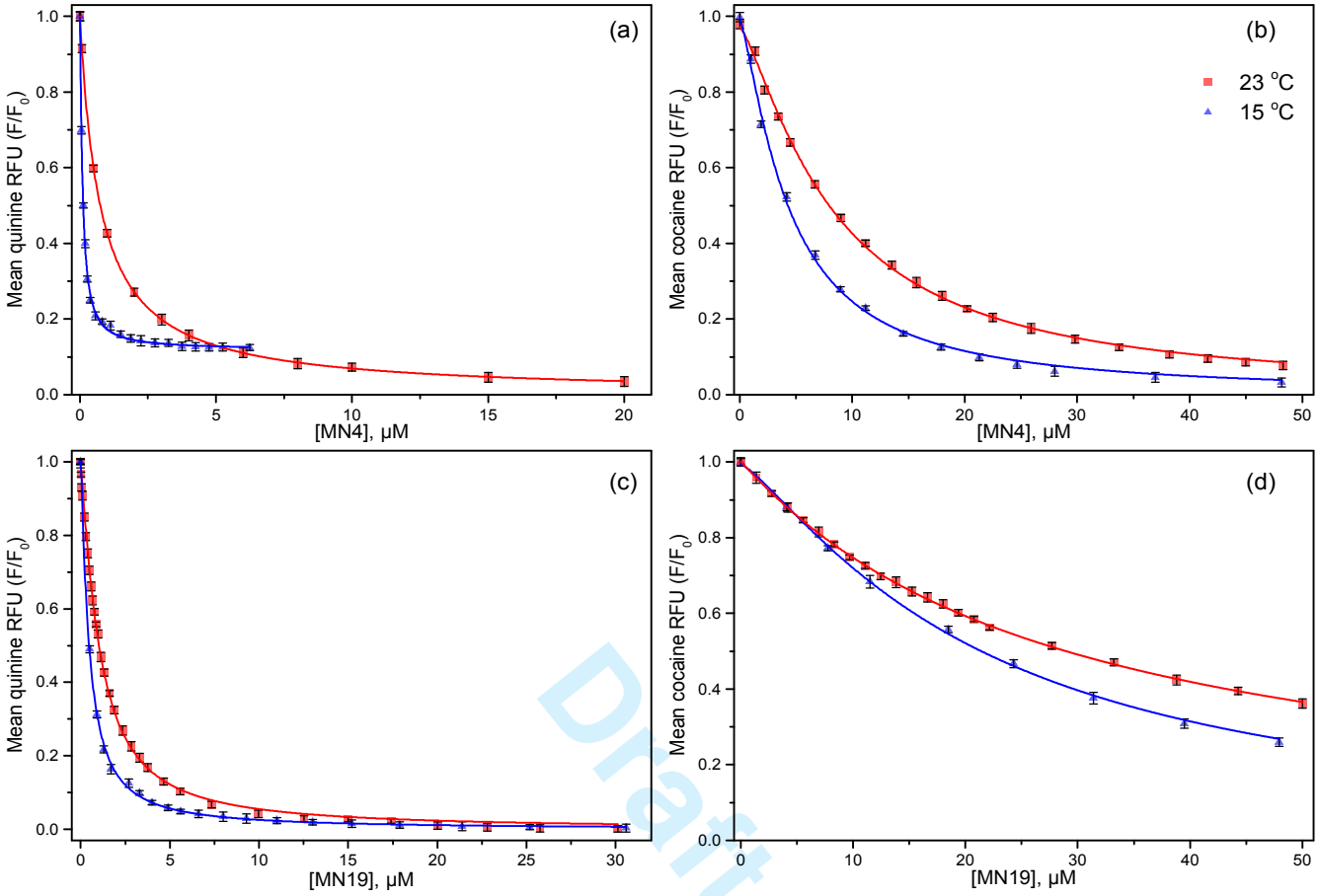
(a)
Mean quinine RFU (F/F0)
[MN4], μM
(b)
23 °C
15 °C
Mean cocaine RFU (F/F0)
[MN4], μM
(c)
Mean quinine RFU (F/F0)
[MN19], μM
(d)
Mean cocaine RFU (F/F0)
[MN19], μM

Figure 3

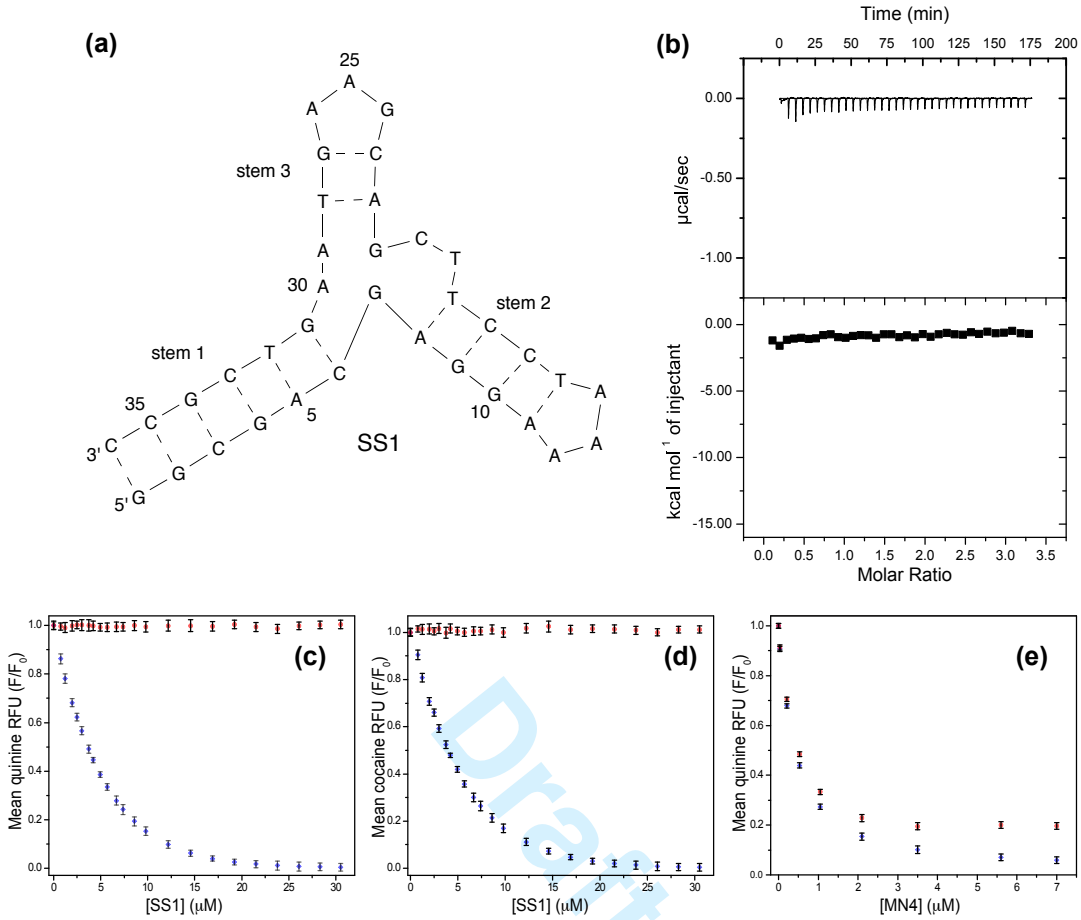

Figure 4

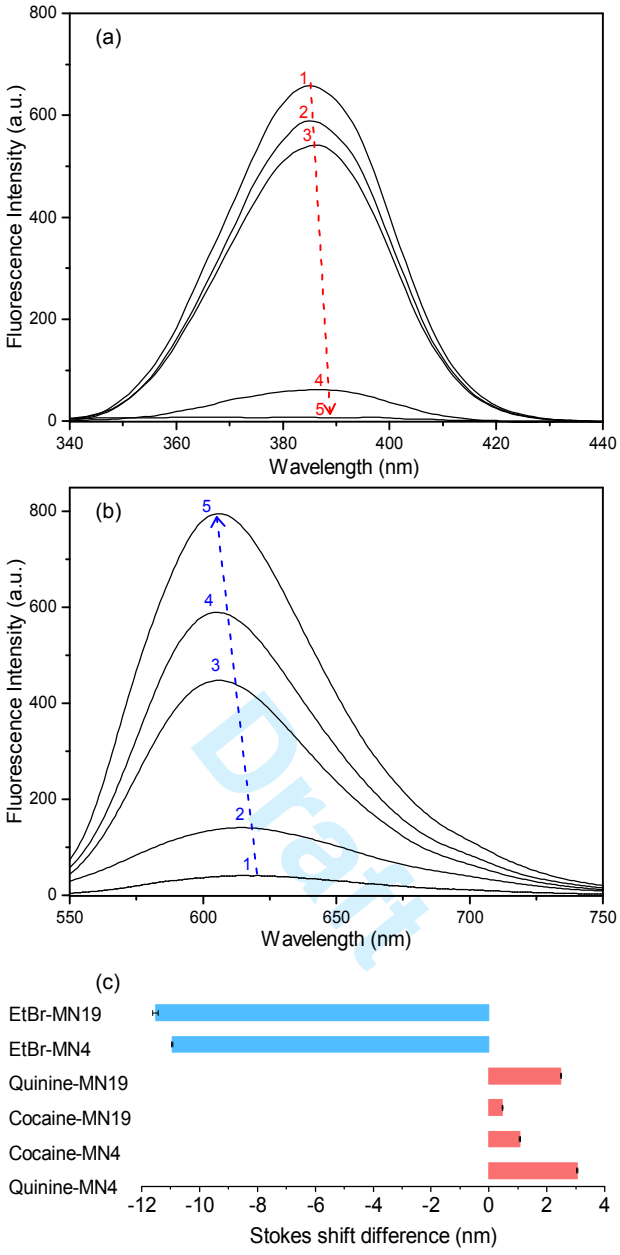
(a)
Fluorescence Intensity (a.u.)
Wavelength (nm)
1
2
3
4
5
(b)
Fluorescence Intensity (a.u.)
Wavelength (nm)
(c)
EtBr-MN19
EtBr-MN4
Quinine-MN19
Cocaine-MN19
Cocaine-MN4
Quinine-MN4
Stokes shift difference (nm)

Figure 5

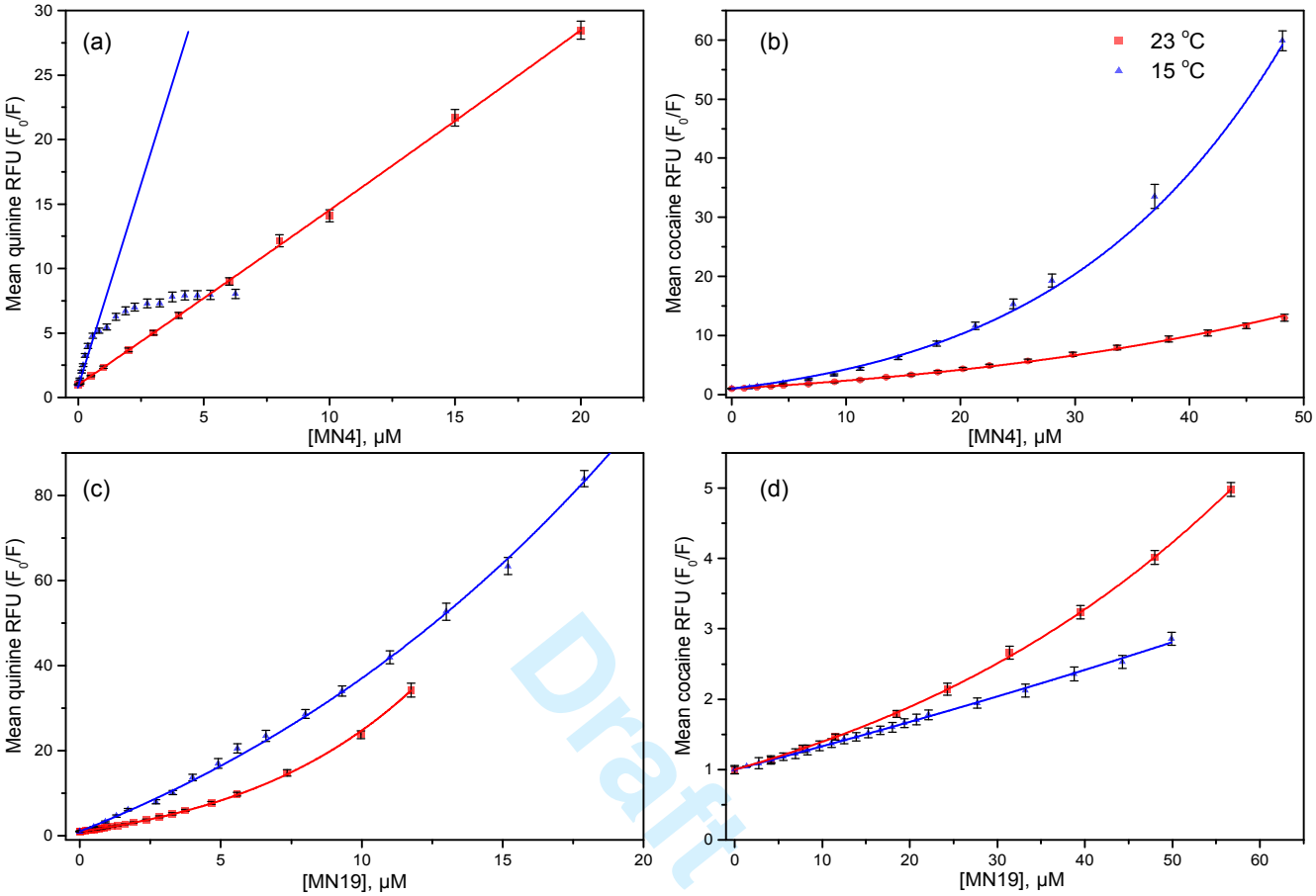
(a)
Mean quinine RFU (F0/F)
[MN4], μM
(b)
23 °C
15 °C
Mean cocaine RFU (F0/F)
[MN4], μM
(c)
Mean quinine RFU (F0/F)
[MN19], μM
(d)
Mean cocaine RFU (F0/F)
[MN19], μM

Figure 6